PCCP

RSC Publishing

PAPER

View Article Online
View Journal | View Issue

Ultrafast photoinduced dynamics of the 3,6-diaminoacridinium derivative ATTO 465 in solution†

Cite this: *Phys. Chem. Chem. Phys.*, 2013, **15**, 1844

Jutta Arden-Jacob,[ab] Karl-Heinz Drexhage,[ab] Sergey I. Druzhinin,[a] Maria Ekimova,[a] Oliver Flender,[a] Thomas Lenzer,*[a] Kawon Oum[a] and Mirko Scholz[c]

The excited state dynamics of the dye ATTO 465, a well-known fluorescence marker for biological applications, have been characterized in various solvents including THF, ethanol, methanol, water and the highly polar protic ionic liquid 2-hydroxyethylammonium formate (2-OH-EAF) by combining results from time-correlated single-photon counting (TCSPC) and ultrafast pump–supercontinuum probe (PSCP) spectroscopy as well as steady-state absorption and fluorescence. In water, 2-OH-EAF and two fluorinated alcohols, there is a pronounced blue-shift and broadening of the $S_0 \rightarrow S_1$ absorption band and also a larger Stokes shift than in the other solvents, indicating a particular influence of hydrogen-bonding interactions. S_1 lifetimes from TCSPC at 25 °C range from 3.3 ns to 5.6 ns. An unusual increase in the S_1 lifetime with temperature is observed for ethanol and methanol, however water behaves in the opposite way. The behavior can be tentatively explained by a solvent- and temperature-dependent ''proximity effect'', where coupling of the close-lying S_1 and S_2 states influences the intramolecular relaxation rate of the dye. In addition, temperature-dependent complex equilibria of ATTO 465 with solvent molecules may influence the measured lifetimes. Several excited-state absorption (ESA) transitions are identified in the PSCP spectra, which are in good agreement with the position of the UV bands in the steady-state absorption spectra. Small shifts of the stimulated emission and ESA bands are consistent with solvation dynamics in the excited electronic state. An additional ~16 ps component in water, visible over the entire spectral range, is tentatively ascribed to a fast IC channel which is accessed by a fraction of ATTO 465 molecules.

Received 3rd October 2012,
Accepted 28th November 2012

DOI: 10.1039/c2cp43493h

www.rsc.org/pccp

1. Introduction

Cationic dyes derived from proflavine (= 3,6-diaminoacridine) are used as an important class of DNA intercalators and as fluorescence markers for microscopic investigations of biological samples. Fig. 1 contains the structure of the dye ATTO 465 used in this study and the ring-nitrogen protonated form of the heterocycle proflavine, which represents the prototype of this dye class.[1–3] The knowledge of the photophysics of such dyes in solution is a prerequisite for a better understanding of their dynamics in more complex environments such as DNA or proteins. Alkyl substitution at the 1-position in the case of ATTO 465, which was originally introduced to allow for facile coupling with biological molecules of interest, has the extra benefit that a well-defined stable cationic dye system is generated. This way, potential complications *e.g.* due to acid–base equilibria as in the case of diluted dye solutions of protonated proflavine are avoided.

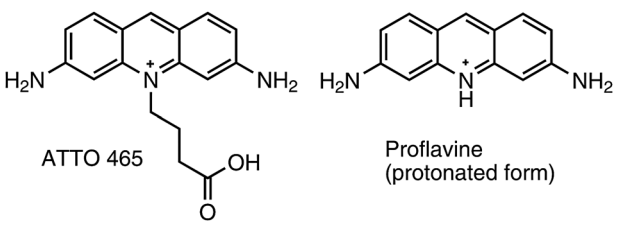

Fig. 1 Chemical structures of ATTO 465 (counter anion in the current study ClO_4^-) and the protonated form of proflavine.

[a] *Universität Siegen, Physikalische Chemie, Adolf-Reichwein-Str. 2, 57076 Siegen, Germany. E-mail: lenzer@chemie.uni-siegen.de, oum@chemie.uni-siegen.de; Fax: +49 271 740 2805; Tel: +49 271 740 2803*
[b] *ATTO-TEC GmbH, Am Eichenhang 50, 57076 Siegen, Germany*
[c] *Max-Planck-Institut für Biophysikalische Chemie, Am Fassberg 11, 37077 Göttingen, Germany*

† Electronic supporting information (ESI) available: Steady-state absorption coefficient spectra of ATTO 465 in ethanol, methanol and water; normalized absorption and fluorescence spectra of ATTO 465 in all solvents; comparison of PSCP spectra for ATTO 465 in water, THF and ethanol; comparison of single wavelength transient absorption signals in water for different concentrations of ATTO 465. See DOI: 10.1039/c2cp43493h

Another interesting feature of ATTO 465 is its Stokes shift, which is considerably larger in water than in less polar solvents such as alcohols. This shift is also much larger than for related molecular fluorescence probes in water, such as ATTO 495, which features two *N*,*N*-dimethylamino groups instead of the two amino groups.[4] The reason for this behavior is not yet understood and therefore requires experimental studies. In addition, the behavior of such molecular probes in ionic liquids (ILs) is of interest, because these media have recently attracted considerable attention as task-specific solvents for biological applications such as peptide and protein folding.[5,6] In the current studies we include the protic ionic liquid (PIL) 2-hydroxyethylammonium formate, which is highly polar[7] and a promising candidate for such biological applications. We present a comprehensive investigation of the dye ATTO 465 in a range of solvents using time-correlated single-photon counting (TCSPC) measurements, ultrafast transient absorption spectroscopy, as well as steady-state absorption and fluorescence. We complement our experiments by DFT/TDDFT calculations for a better understanding of the structure, energetics and photophysics of ATTO 465.

2. Experimental

2.1 Steady-state absorption and fluorescence spectra

Steady-state absorption spectra of the ATTO 465 dye in different solvents were measured on Varian Cary 5000 and Perkin Elmer Lambda 750 spectrometers with baseline correction. Fluorescence spectra were recorded using Varian Cary Eclipse and Horiba Jobin-Yvon Fluorolog-3 spectrometers. Samples were excited at or close to the absorption maximum. The fluorescence raw data were corrected for the instrument response function. Fluorescence quantum yields of ATTO 465 in several solvents were determined using quinine sulfate in 1 N H_2SO_4 as standard (Φ_f = 0.546 at 25 °C).[8]

2.2 Time-correlated single photon counting (TCSPC)

One of our TCSPC systems was already described at length in previous publications.[9–11] Briefly, a solution of ATTO 465 in the solvent of interest was prepared with an optical density of 0.1–0.3 at the $S_0 \rightarrow S_1$ absorption band maximum in a 10 mm × 10 mm quartz cuvette, which was placed in a temperature-controlled sample holder (±0.05 °C). The solution was then thoroughly bubbled with N_2 and excited using a pulsed nitrogen flash lamp (FWHM 2 ns, 297 nm, repetition rate 50 kHz). Experiments were performed in the range 25.0–65.0 °C (methanol), 25.0–75.0 °C (ethanol), 25.0–95.0 °C (water), and at 25 °C for THF and 2-hydroxyethylammonium formate (2-OH-EAF). Fluorescence was recorded at the maximum of the emission band. Decay curves were deconvolved with the instrument response function (IRF), recorded using a Ludox solution, which resulted in highly reproducible monoexponential decays over typically two to three orders of magnitude. Standard deviations for a set of TCSPC data (typically consisting of 4–8 measurements) were *ca.* ±20 ps, except for the IL (*ca.* ±200 ps), because in that case superimposed impurity fluorescence increased the uncertainty in the determination of the ATTO 465 lifetime. In the case of the temperature-dependent experiments, lifetimes obtained at 25 °C before starting and after finishing the temperature series were identical.

In addition, fluorescence decay curves of ATTO 465 were recorded on another TCSPC setup (Horiba Jobin-Yvon TemPro, time calibration 55 ps per channel, software: DataStation 2.5, DAS6.4) at room temperature using $S_0 \rightarrow S_1$ excitation at 454 nm (Horiba Jobin-Yvon NanoLED-460, FWHM 1.1 ns, repetition rate 1 MHz). Ethanol and water (both undeuterated and deuterated), formamide, dimethylformamide (DMF), 2,2,2-trifluoroethanol (TFE) and 1,1,1,3,3,3-hexafluoropropan-2-ol (HFP) were employed as solvents. Deconvolution was performed using an IRF recorded with a Ludox AS-40 solution (Sigma-Aldrich) in water, leading to pure monoexponential decays over three orders of magnitude. The estimated accuracy of these lifetime values is *ca.* ±50 ps. Typically, the integral fluorescence of the sample was collected. In the case of water, HFP and formamide, comparisons were also made with measurements, where an interference filter (514 nm, bandwidth ±5 nm) was employed, resulting in identical lifetime values. For water, the lifetime of ATTO 465 was also measured at different pH values: at pH 4 in a citrate buffer (Sigma-Aldrich 33643), at pH 4.1 in a diluted acetic acid solution, at pH 7.4 in a PBS buffer containing 0.137 M NaCl, 0.0027 M KCl, 0.0018 M KH_2PO_4 and 0.0090 M KH_2PO_4, at pH 10 in a borate buffer (Merck Titrisol 1.09890.0001) and at pH 10.3 in a diluted KOH solution.

We also note that the results for the solvents water, methanol and ethanol, measured with the two different excitation wavelengths 297 and 454 nm on two different setups, are in complete agreement.

2.3 Pump–SuperContinuum Probe (PSCP) spectroscopy

Ultrafast broadband absorption spectroscopy based on the PSCP technique[12] in the range 340–770 nm was performed using our setup described previously.[11,13–15] ATTO 465 was excited at 489 nm (ethanol) or 481 nm (THF, water). Transient spectra for each pump–probe delay were accumulated over 1500 laser shots employing single-shot baseline correction. For the final representation, typically 5–10 transients around a given time delay were averaged. The pump–probe intensity cross-correlation time in the current experiments was 60–90 fs and the time accuracy 10 fs.

2.4 Chemical substances

The dye ATTO 465 (with dominant (>90%) counter anion ClO_4^-) was used without further purification. No signs of degradation were detected in any of the experiments reported below. Solvents had a specified purity of 99% or better (*ca.* >97% in the case of the protic ionic liquid). The measurements were carried out in thoroughly N_2-bubbled solutions or – where stated – in air-saturated solutions. In all experiments the dye concentration was in the range 10^{-4} to 10^{-6} mol L^{-1}.

3. Theoretical calculations

The equilibrium structure of the ground electronic state of ATTO 465 was optimized by density functional theory (DFT)

using the B3LYP functional[16] and a 6-311+G(d,p) basis set. Time-dependent density functional theory (TDDFT)[17,18] was then applied to these geometries for calculating the first five excited singlet electronic states using the B3LYP functional and a 6-31+G(d) basis set. The PCM solvent model was employed for water. Calculations were carried out using the Gaussian 09 package.[19] Detachment–attachment electron density plots were obtained using Q-Chem 3.0.[20]

4. Results and discussion

4.1 Steady-state absorption and fluorescence of ATTO 465

Fig. 2 shows absorption spectra (left side) and fluorescence spectra (right side) for the solvents ethanol, methanol, water, THF and 2-OH-EAF studied in detail in the current experiments. Complete absorption coefficient spectra down to 200 nm for ethanol, methanol and water can be found in Fig. S1 of the ESI.† Characteristic quantities and relevant solvent properties[7,21–23] are summarized in Table 1. Absorption and fluorescence spectra in additional solvents can be found in Fig. S2 and S3 (ESI†), respectively.

The absorption spectra in THF, ethanol and methanol are centered at *ca.* 465 nm and exhibit a shoulder to the blue, with a spacing of about 1350 cm^{-1}. In a previous study employing surface-enhanced resonance Raman scattering of proflavine, strong vibrational bands at 1322, 1362 and 1391 cm^{-1} were reported, which is consistent with the spacing found for ATTO 465.[24] The relatively unstructured appearance of the whole spectrum is likely due to additional lower-frequency modes (594, 648, 758, 352 and 412 cm^{-1}).[24] The peak of the absorption spectrum in water (ε = 80.1) and 2-OH-EAF (ε = 57.3)[7] is blue-shifted by about 500 and 1000 cm^{-1}, respectively, and the spectra are significantly broadened. While this suggests, that increased polarity might be the reason for these effects, we note that even stronger blue-shifts of the absorption spectra are found for the fluorinated alcohols TFE (ε = 27.7) and HFP (ε = 16.7), which both have a significantly smaller dielectric constant than water and the IL, see Table 1 and Fig. S2 (ESI†). Possible reasons for this behavior will be discussed further below.

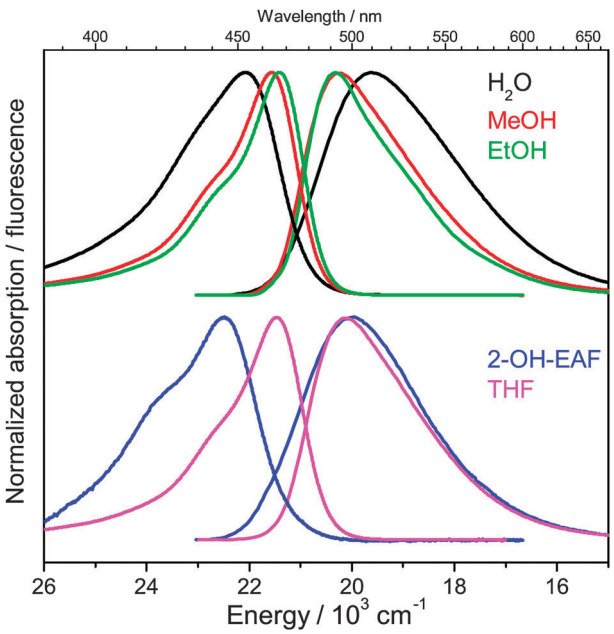

Fig. 2 Steady-state absorption and fluorescence spectra of ATTO 465 in (top) ethanol, methanol and water, and (bottom) THF and the ionic liquid 2-hydroxyethylammonium formate (2-OH-EAF).

The fluorescence spectra in Fig. 2 show only a fairly small Stokes shift in methanol, ethanol and THF in the range 1100–1350 cm^{-1}. It is considerably larger in water and 2-OH-EAF (*ca.* 2500 cm^{-1}), and also in the two fluorinated alcohols (Table 1). This difference is surprisingly large compared to *e.g.* other acridinium dyes featuring dimethyl substitution at both amino groups.[4] Similar to the absorption spectra, the width of the fluorescence spectra is considerably larger in water, 2-OH-EAF, TFE and HFP compared to the other solvents listed in Table 1.

4.2 DFT/TDDFT calculations for ATTO 465

For a basic understanding of the absorption spectra in Fig. 2, transition energies for the first five singlet electronic states in the gas-phase and in water (PCM model) were calculated, including oscillator strengths for the gas-phase case (Table 2). As can be clearly seen, the strong band in Fig. 2 can be assigned to $S_0 \rightarrow S_1$, which is the only bright transition in this spectral region (compare also Fig. S1, ESI†) and corresponds to predominantly HOMO $\rightarrow$ LUMO excitation, with a small (*ca.* 6%) admixture of HOMO $-$ 1 $\rightarrow$ LUMO + 1. The solvent influence on the band position is relatively weak, resulting in a 13 nm red-shift. We note that the calculations deviate from the experimentally determined band position by 48 nm (Tables 1 and 2). Such an overestimation of the experimental transitions by TDDFT approaches has been found previously for cyanines and acridines, independent of the functional used. The reason for the deviations is thought to be the multideterminantal structure of these systems, especially in the case of extended conjugated systems.[25–27] The 3,6-diaminoacridinium system of ATTO 465 features a similar chromophore, and the deviations between the TDDFT results and experimental spectra are therefore not surprising. Still, we believe that such calculations can provide at least a qualitative description of the state ordering and energy levels in this system.

The detachment–attachment electron density plots in Fig. 3 show that electron density is redistributed within the central part of the ring system upon $S_0 \rightarrow S_1$ excitation. In addition, electron density is slightly reduced at the two amino groups. We also note that the ring system is not completely planar but exhibits a slight "concave" curvature toward the side on which the alkyl chain resides. Close in energy to the S_1 state, there is an almost "dark" electronic state, which corresponds to a HOMO $-$ 1 $\rightarrow$ LUMO transition. This state could potentially couple to S_1, for a further discussion see Section 4.5.

4.3 Fluorescence lifetimes and quantum yields for ATTO 465

We also investigated solvent effects on the measured excited state lifetimes and quantum yields of the dye. A representative TCSPC trace for ATTO 465 in water at 25 °C can be found in Fig. 4.

Table 1 Summary of steady-state absorption and fluorescence data (at 23 °C) as well as quantum yield and lifetime data (at 25 °C) of ATTO 465 in different solvents

Solvent	EtOH	MeOH	H_2O	THF	2-OH-EAF[a]	EtOD	TFE[b]	HFP[c]	D_2O	Formamide	DMF
$\lambda^{a}_{max,1}$[d]/nm	467	464	453	466	445	467	451	447	453	463	470
$\tilde{\nu}^{a}_{max,1}$[e]/cm^{-1}	21 410	21 560	22 070	21 470	22 490	21 410	22 190	22 380	22 070	21 600	21 300
$\varepsilon_{max,1}$[f]/M^{-1} cm^{-1}	65 500	65 400	42 700	—	—	—	—	—	—	—	—
$\lambda^{a}_{max,2}$[g]/nm	263	262	263	264	—	—	—	—	—	—	—
$\tilde{\nu}^{a}_{max,2}$[h]/cm^{-1}	38 060	38 120	38 020	37 940	—	—	—	—	—	—	—
$\varepsilon_{max,1}/\varepsilon_{max,2}$[i]	1.10	1.07	0.86	0.93	—	—	—	—	—	—	—
λ^{f}_{max}[j]/nm	491	493	507	496	497	492	500	494	507	501	497
$\tilde{\nu}^{f}_{max}$[k]/cm^{-1}	20 320	20 230	19 600	20 110	20 000	20 270	20 130	19 930	19 600	19 860	20 060
$(\tilde{\nu}^{a}_{max,1}-\tilde{\nu}^{f}_{max})$[l]/$cm^{-1}$	1090	1330	2470	1360	2490	1140	2060	2450	2470	1740	1240
$FWHM_a$[m]/cm^{-1}	1600	1750	2360	1760	2410	1600	2000	2100	2360	2070	1730
$FWHM_f$[n]/cm^{-1}	2170	2420	3070	2430	2770	2250	3080	2870	2960	2690	2290
τ[o]/ps	4030	4430 4040[p]	5220 5130[p]	3940	5110	3860[p]	5190[p]	5570[p]	5610[p]	4160[p]	3310[p]
Φ_f[q]	0.65	0.59 0.54[p]	0.49 0.48[p]	0.53	—	—	—	—	—	—	—
k_r[r]/ns^{-1}	0.16	0.13 0.13[p]	0.094 0.094[p]	0.14	—	—	—	—	—	—	—
k_{nr}[s]/ns^{-1}	0.088	0.092 0.11[p]	0.098 0.10[p]	0.12	—	—	—	—	—	—	—
σ^{max}_{em}[t]/10^{-16} cm^2	1.17	0.91	0.55	0.83	—	—	—	—	—	—	—
$\mu(S_1 \rightarrow S_0)$[u]/D	5.33	5.08	4.45	4.67	—	—	—	—	—	—	—
$\mu(S_0 \rightarrow S_1)$[v]/D	6.31	6.52	6.05	—	—	—	—	—	—	—	—
β[w]	0.75	0.66	0.47	0.55	—	0.75	0.00	0.00	0.47	0.48	0.69
ε[x]	25.3	33.0	80.1	7.5	57.3	25.3	27.7	16.7	79.7	111	37.6

[a] 2-Hydroxyethylammonium formate. [b] 2,2,2-Trifluoroethanol. [c] 1,1,1,3,3,3-Hexafluoropropan-2-ol. [d] Wavelength of $S_0 \rightarrow S_1$ absorption maximum. [e] Wavenumber of $S_0 \rightarrow S_1$ absorption maximum. [f] Peak absorption coefficient of the $S_0 \rightarrow S_1$ band with an accuracy of *ca.* ±3%. [g] Wavelength of UV band absorption maximum. [h] Wavenumber of UV band absorption maximum. [i] Ratio of peak absorption coefficients for the two bands. [j] Wavelength of fluorescence maximum. [k] Wavenumber of fluorescence maximum. [l] Stokes shift. [m] Full width at half-maximum of the $S_0 \rightarrow S_1$ absorption band. [n] Full width at half-maximum of the $S_1 \rightarrow S_0$ fluorescence band. [o] Lifetime from TCSPC. [p] In air-saturated solution. [q] Fluorescence quantum yield. [r] Radiative rate constant. [s] Nonradiative rate constant. [t] Emission cross-section at maximum. [u] Transition dipole moment for emission. [v] Transition dipole moment for absorption. [w] Kamlet–Taft parameter β for the hydrogen bond accepting ability ("basicity")[21,22] of the solvent. [x] Dielectric constant.[7,23]

Table 2 Results of DFT/TDDFT calculations (B3LYP functional) for the first 5 vertical electronic transitions of ATTO 465 in the gas phase and in water, and oscillator strengths *f* from the gas-phase calculations

$S_0 \rightarrow S_n$	λ /nm (gas phase)	λ /nm (water)	*f*
1	392	405	0.55
2	388	392	0.02
3	293	290	0.00
4	288	282	0.00
5	283	269	0.00

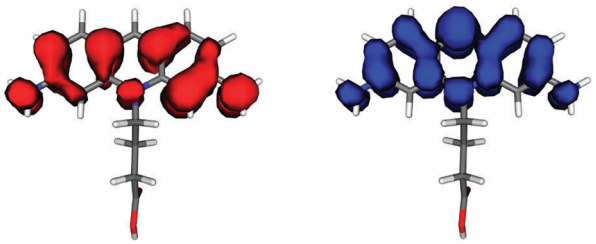

Fig. 3 Detachment density (left) and attachment density (right) for the $S_0 \rightarrow S_1$ transition of ATTO 465 obtained from the DFT/TDDFT calculations.

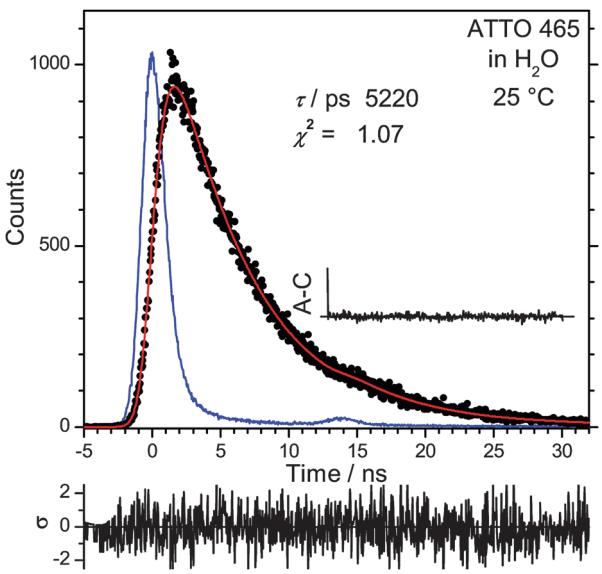

Fig. 4 Representative time-correlated single photon counting decay (black circles) for ATTO 465 in H_2O at 25 °C. Excitation: 297 nm, detection: 510 nm. The red line represents the best fit with τ = 5220 ps (χ^2 = 1.07) using the instrument response function obtained from a Ludox scattering solution (blue line). Inset: autocorrelation (A–C) trace, lower plot: weighted residuals.

No changes in the lifetime were observed in a study of the concentration dependence in water in the range 2×10^{-7}–3×10^{-6} M. Lifetimes are summarized in Table 1. They are averages over 4–8 individual experiments and are well described by single exponential decays. A systematic increase in fluorescence lifetime is observed in the sequence THF < ethanol < methanol < 2-OH-EAF < water.

A lifetime comparable to water is also found for ATTO 465 in fluorinated alcohols, whereas in formamide and DMF lifetimes are comparable to THF, ethanol and methanol (Table 1). Deuteration of water increases the lifetime of ATTO 465. As expected, in aerated solutions, oxygen quenches the fluorescence, leading to a lifetime reduction of ~400 ps in methanol and ~100 ps in water. The difference is most likely due to the higher oxygen solubility in methanol.[28]

We note that the solvent dependent increase in the lifetime of ATTO 465 is in marked contrast to previous results of Natarajan and co-workers for 3,6-diaminoacridinium: they reported TCSPC experiments (with a claimed time resolution of 50 ps) showing single exponential decays with a virtually solvent-independent fluorescence lifetime of (4.6 ± 0.2) ns (see *e.g.* Table 1 and Fig. 2 in their paper).[3] However, they observe multiexponential transients in their fluorescence up-conversion experiments, which have largely decayed after 500 ps (see their Fig. 3). The shape of their upconversion signals also does not agree with the fit results for these transients, where a dominant component in the range 4.4–4.8 ns with an amplitude of typically in the range of more than 80% was claimed (see Tables 2 and 3 in their paper). Thus it must be concluded that their experimental results are not internally consistent.[3] We therefore refrain from including these data in the further discussion.

In addition, we measured fluorescence quantum yields Φ_f using quinine sulfate as standard.[8] From these and the measured lifetimes τ, the radiative and nonradiative rate constants $k_r = \Phi_f/\tau$ and $k_{nr} = (1 - \Phi_f)/\tau$, respectively, were determined. All values are summarized in Table 1. Focusing on the protic solvents, Φ_f systematically decreases from ethanol (65%) toward methanol (59%) and water (49%). Looking at the rate constants, the value of k_r varies more strongly than k_{nr}. The considerable reduction of k_r from ethanol to water is quite surprising, because very often radiative rates are assumed to be practically solvent independent and changes in the rates of nonradiative processes are believed to be more important.[29] Quite peculiar behavior of ATTO 465 is also observed, when recording the temperature dependence of the fluorescence lifetime in ethanol, methanol and water (Fig. 5). While water shows the "normal" trend, *i.e.*, a reduction of the lifetime with increasing temperature, the two alcohols show the opposite trend, namely a weak systematic increase in the lifetime. This behavior of ATTO 465 in methanol and ethanol is quite unusual, because nonradiative processes such as internal conversion from an excited electronic state are typically accelerated due to the higher average vibrational energy of the molecules at higher temperatures.[29–32] In addition, the dielectric constant of methanol and ethanol decreases quite substantially with increasing temperature,[33] which should, in the current case, also favor a decrease in lifetime (note that the mid-polar THF has a smaller τ, see Table 1). However, the opposite trend is observed. Possible interpretations will be discussed below.

We note that an influence of temperature-dependent acid–base equilibria on the lifetime of ATTO 465 is unlikely. In experiments at 25 °C for pH 4.1 (diluted acetic acid) and for pH 10.3 (diluted KOH solution) we found single exponential decays

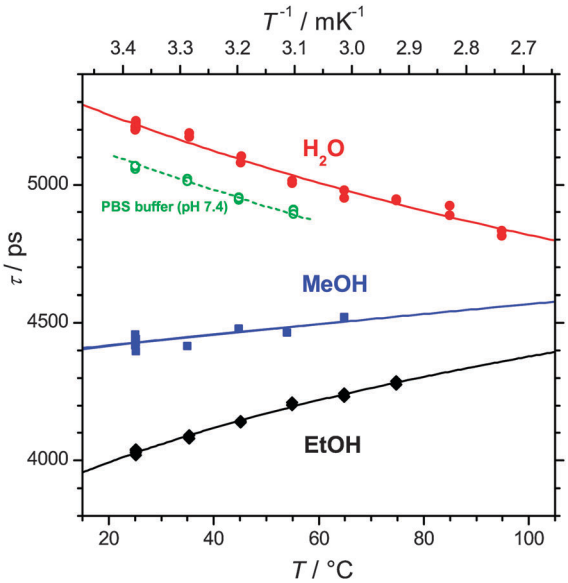

Fig. 5 Temperature-dependent fluorescence lifetimes of ATTO 465 in ethanol (black), methanol (blue) and water (red) from time-correlated single photon counting measurements. The green open symbols are for ATTO 465 in a PBS buffer at pH 7.4. Solid and dashed lines are intended merely as a guide to the eye.

with lifetimes of 5120 and 5170 ps, respectively (compare the value of 5220 ps from Table 1). The steady-state absorption and fluorescence spectra did not change for these two solutions. We therefore believe that acid–base equilibria involving the carboxyl and the two amino groups of ATTO 465 have a negligible effect in the current measurements. We note however that the use of buffer solutions had a visible influence on the decays. In the case of citrate (pH 4), the lifetime was reduced to 4920 ps at 25 °C. For the borate buffer, the fit provided a lifetime of 5220 ps, yet there was an obvious departure from monoexponential behavior. In the PBS buffer (pH 7.4), a value of 5060 ps was measured at 25 °C. We suspect that the high concentration of ions in these buffers could be the reason for such effects, which might lead to strong Coulomb interactions with the dye and possibly also the formation of ion pairs. In spite of these changes in lifetimes, the trend in the temperature dependence remained robust. This is *e.g.* illustrated by the results for the PBS buffer in Fig. 5, where the curve runs parallel to the one for pure water.

4.4 PSCP experiments and their global analysis

We performed ultrafast broadband transient absorption experiments of ATTO 465 in the solvents THF, ethanol and H_2O to obtain further insight into the relaxation dynamics of the dye. In all cases, solutions were thoroughly bubbled with nitrogen prior to the measurements. A representative result for ethanol is shown in Fig. 6. The top panel shows the development at very early times. Upon approaching $t = 0$, a negative band centered at *ca.* 480 nm with a shoulder in the range 500–550 nm and an absorption band with a peak at 420 nm appear. We assign the three features to S_0 ground state bleaching (GSB), $S_1 \rightarrow S_0$ stimulated emission (SE) and $S_1 \rightarrow S_n$ excited state absorption

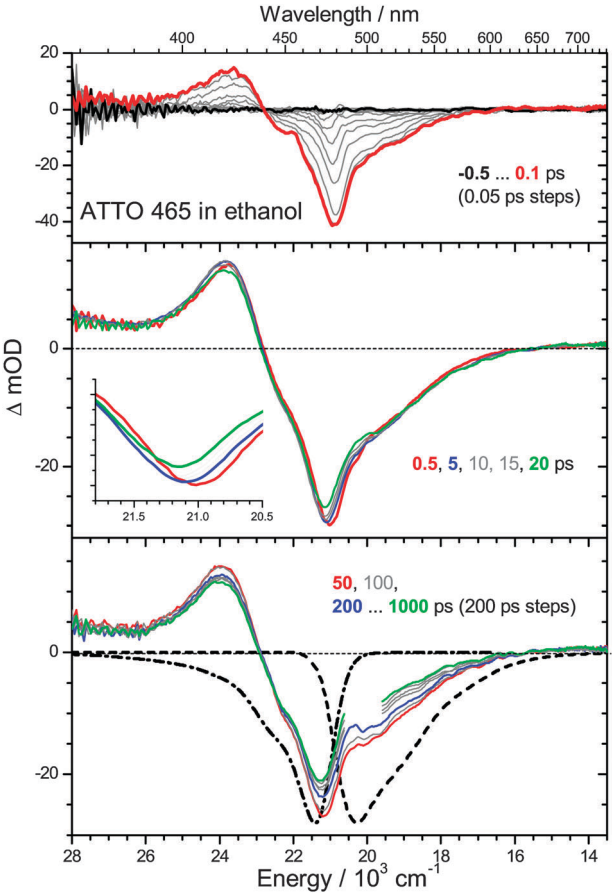

Fig. 6 Transient PSCP absorption spectra of ATTO 465 in ethanol for excitation at λ_{pump} = 489 nm (colored and grey lines). In the lower panel, the dash-dotted and dashed black lines indicate the inverted steady-state absorption and the steady-state stimulated emission spectrum (calculated from the steady-state fluorescence spectrum). A narrow spectral window around the pump wavelength, which shows excessive noise arising from pump beam straylight, is omitted for some of the spectra for the sake of clarity.

(ESA), respectively. The slightly structured appearance is due to Raman features arising from ATTO 465 during the time overlap of the pump and probe pulses.

The middle panel demonstrates the spectral evolution on intermediate timescales up to 20 ps. In this time range, we observe a slight decrease of the GSB (which becomes more apparent in the inset on the left) and a slight movement of the SE shoulder toward the red. The spectral changes and the timescale are characteristic of the solvent's response to the altered charge distribution of the S_1 state.[34] The small changes are understandable considering the fairly small Stokes shift of ATTO 465 in this solvent (1090 cm^{-1}, see Table 1). A slight spectral movement on the same timescale is also visible on the $S_1 \rightarrow S_n$ ESA band, in this case a blue-shift, which indicates that upon solvent relaxation the upper state in the ESA process is less stabilized than S_1.[14,35] We also note that there is a very weak absorption visible above 650 nm which must be assigned to another ESA band originating from S_1.

On long timescales up to 1 ns, shown in the bottom panel, we observe first the remainder of the solvent relaxation in the GSB, SE and ESA regions, which is consistent with the slowest part of ethanol's solvation response.[34] Afterwards, in all spectral regions we see a slow uniform decay, which is consistent with the lifetime extracted from our TCSPC experiment (4030 ps, see Table 1).

All PSCP measurements were treated by a global kinetic analysis.[14,15,36] The following kinetic scheme was considered:

$$\begin{aligned} S_0 &\xrightarrow{h\nu_{Pump}} S_1 \\ S_1 &\xrightarrow{k_r} S_0 \\ S_1 &\xrightarrow{k_{IC}} S_0 \\ S_1 &\xrightarrow{k_{ISC,1}} T_1 \\ T_1 &\xrightarrow{k_{ISC,2}} S_0 \end{aligned} \qquad (1)$$

Bimolecular quenching processes of S_1 by oxygen can be safely neglected for the nitrogen-bubbled solutions employed. Because time-resolved data are only available up to 1 ns pump–probe delay, the S_1 decay rate $k = \tau^{-1} = k_r + k_{IC} + k_{ISC,1}$ was fixed at the value determined from the TCSPC experiments (Table 1). The second ISC step is typically in the μs to ms range (*i.e.* $k_{ISC,2} \ll k$) and depends on the specific amount of oxygen in the solution. In the current case, with very low amounts of oxygen, bimolecular quenching is expected to be slow, and we expect time constants of the triplet quenching in the range of milliseconds. Therefore, the recovery of S_0 population described by the kinetic system in eqn. (1) will be biexponential, with one component given by τ (Table 1) and a very slow component given by $\tau_{ISC,2}$. In the PSCP experiments, the entire spectrum has uniformly decayed to about 80% of its initial amplitude within 1 ns. This suggests that only a minor fraction of the S_1 population decays to triplets (on the order of $\leq$10%, as estimated from the noise level of the spectra). This is consistent with previous measurements.[4] In agreement with this finding, up to 1 ns we do not see any build-up of triplet absorption: for a related system (protonated proflavine) an extinction coefficient of 6000 M^{-1} cm^{-1} for $T_1 \rightarrow T_n$ was reported (peak at 455 nm),[37] which is considerably smaller than $\varepsilon_{max,1}$ of $S_0 \rightarrow S_1$ (Table 1) and $S_1 \rightarrow S_n$. It is therefore understandable that triplet absorption is not detected by PSCP even at 1 ns delay time, because it has a very small amplitude and also overlaps with strong bleach features (see Fig. 6). For the global modeling, a time-dependent[14,15,36] S_1 spectrum was assumed, where transient spectral changes, such as shifts of the SE and ESA bands can be conveniently modeled.

Fig. 7 contains representative fits to experimental PSCP spectra in (A) ethanol and (B) water after solvent relaxation has ceased. The simulated PSCP spectrum is shown as a black line consisting of a superposition of S_0 (red) and S_1 contributions (blue). The S_1 spectrum consists of SE in the range 480–650 nm (both solvents) and three ESA features: a strong one centered at around 420 nm (400 nm) in ethanol (water), a weak one rising just at the lower limit of the covered

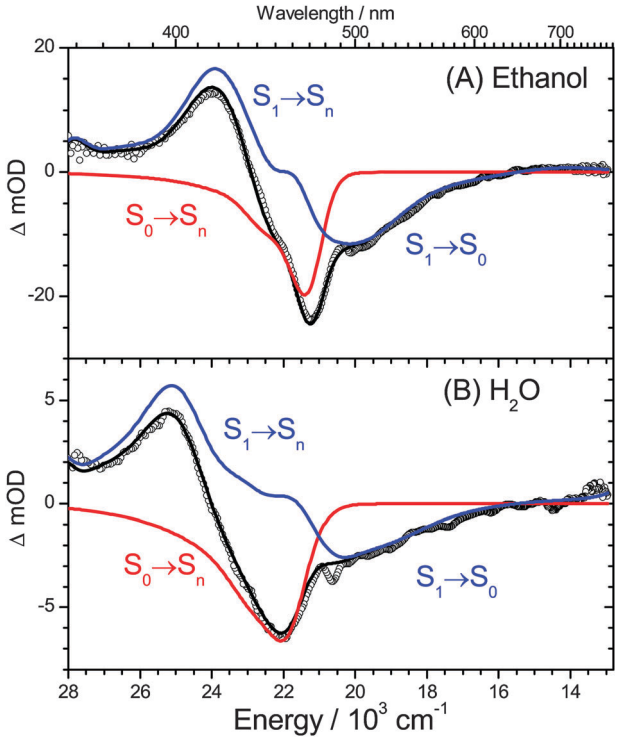

Fig. 7 Species-associated spectra of ATTO 465 in (A) ethanol at a time delay of 200 ps and (B) water at a time delay of 215 ps from global kinetic analysis. (Open circles) experimental spectrum. (Black lines): result from global kinetic analysis with contributions from $S_0 \rightarrow S_n$ GSB (red lines) and combined $S_1 \rightarrow S_n$ ESA and $S_1 \rightarrow S_0$ SE (blue lines).

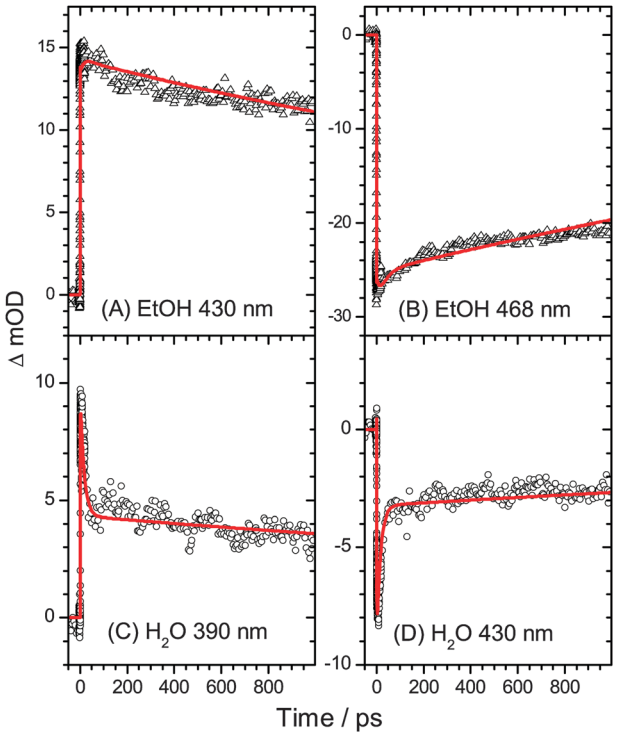

Fig. 8 Representative kinetic traces for ATTO 465 in different protic solvents: (A) and (B) ethanol at 430 nm and 468 nm. (C) and (D) Water at 390 and 430 nm, respectively. Solid red lines are results from global analysis.

wavelength range (*ca.* 360 nm) and a weak tail above 650 nm. An unambiguous decomposition of ESA and SE contributions is difficult: from the steady-state absorption spectrum in Fig. S1 (ESI†), one can deduce that there might be up to five ESA bands present over the wavelength range covered by PSCP. They could be centered at around ~390, 470, 600, 720 and 840 nm (taking, *e.g.*, the bands for ATTO 465 in ethanol at ~210, 230, 260, 280 and 300 nm in Fig. S1 (ESI†) as possible final S_n states for ESA transitions from S_1). For instance, the weak ESA above 650 nm clearly indicates that there must be such a transition somewhere in the red to near-IR spectral region.

In Fig. 8, we show selected kinetic traces for the protic solvents ethanol (A, B) and water (C, D) together with the results from the global analysis (solid red lines). For ethanol, we observe a weak curvature in the early part of the kinetics, which is also present for transients in other spectral regions (not shown here). The curvature can be explained by solvation dynamics with known time constants from the literature (0.03, 0.39, 5.03 and 29.6 ps).[34] The final slow decay of the transient is fitted well by the 4.0 ns time constant independently determined by TCSPC.

For water, it is well known that its solvation dynamics are very fast and can be described by a multiexponential solvent relaxation function (time constants 0.112, 0.30 and 1.45 ps).[38] The curvature in the transients at early times (not shown here) can be well described by such a function and is consistent with the one seen in ref. 38 for a range of molecular probes. However, surprisingly, for ATTO 465 in water there is another slower component of roughly ~16 ps which is visible at all wavelengths and describes a decay of the spectrum with a substantial amplitude. This will be discussed further below. Finally, the entire spectrum decays with a time constant consistent with the TCSPC measurement (5.2 ns, Table 1).

The spectral decay behavior of ATTO 465 in THF is comparable to that in ethanol. The PSCP spectra exhibit a similar spectral shape except for some minor blue-shift in the case of THF (Fig. S4, ESI†). As expected, the solvation dynamics in THF are much faster, and can be well fitted by time constants from the literature (0.228 and 1.52 ps).[34] A minor narrowing of the S_1 ESA band with a time constant of 11.5 ps is assigned to deactivation of vibrationally hot ATTO 465 molecules in S_1 by collisions with the solvent, in agreement with time constants for other organic molecules such as carotenoids and azulene obtained from previous studies of collisional relaxation in the ground electronic state.[15,36,39] The component might be also present in ethanol, but it is not possible to unambiguously assign this process because of the additional solvation dynamics present in that case.

4.5 Photophysical peculiarities of ATTO 465

Three experimental observations for ATTO 465 deserve further discussion: firstly, the steady-state absorption spectra in water, 2-OH-EAF (Fig. 2) and the two fluorinated alcohols (Fig. S2, ESI†) are considerably blue-shifted and the Stokes shift is larger compared to *e.g.* ethanol (Table 1). Secondly, the increase in the

S_1 lifetime with increasing temperature in ethanol and methanol is notable, whereas this lifetime decreases in water (Fig. 5). Thirdly, the ~16 ps spectral decay component with large amplitude in water is distinctly different from the other two solvents (see *e.g.* ethanol in Fig. 8).

We consider first the blue-shift of the ATTO 465 steady-state absorption spectra in water, 2-OH-EAF, TFE and HFP relative to methanol/ethanol. The results for the two fluorinated alcohols suggest that this cannot be due to a simple systematic polarity effect influencing the energy gap between S_1 and S_0. A tentative explanation might be found on the basis of a Kamlet–Taft approach: a reasonable correlation can be obtained when the $S_0 \rightarrow S_1$ absorption maxima are plotted against the Kamlet–Taft parameter β (Table 1), which describes the hydrogen bond accepting ability (= "basicity") of a solvent.[21,22] In fact, the correlation in Fig. 9 is qualitatively similar to those for "β-sensitive" Kamlet–Taft probes, such as the ABF dye (= 3-(4-amino-3-methyl-phenyl)-7-phenyl-benzo-[1,2-b:4,5-b′]-difuran-2,6-dione).[40]

Therefore, we believe that the trends in the absorption maxima can be most likely traced back to considerable structural differences of the solvent network, especially with respect to the hydrogen-bond arrangement of ATTO 465 in S_0 and S_1. This results in a non-optimal arrangement of solvent molecules in S_1 after Franck–Condon excitation. After solvent relaxation, however *e.g.* the fluorescence in water is more red-shifted than in ethanol or methanol (Fig. 2) indicating a substantial stabilization of S_1 due to solvent rearrangement which is probably accompanied by destabilization of S_0 at this particular solvent configuration. The larger FWHM of both the $S_0 \rightarrow S_1$ absorption and $S_1 \rightarrow S_0$ fluorescence bands (Table 1) might additionally suggest a more inhomogeneous solvent environment in water, 2-OH-EAF and the fluorinated alcohols. Considering the structure of ATTO 465, with two amino groups effectively delocalizing the charge of the central ring-nitrogen atom *via* the conjugated system, the occurrence of such effects appears to be understandable.

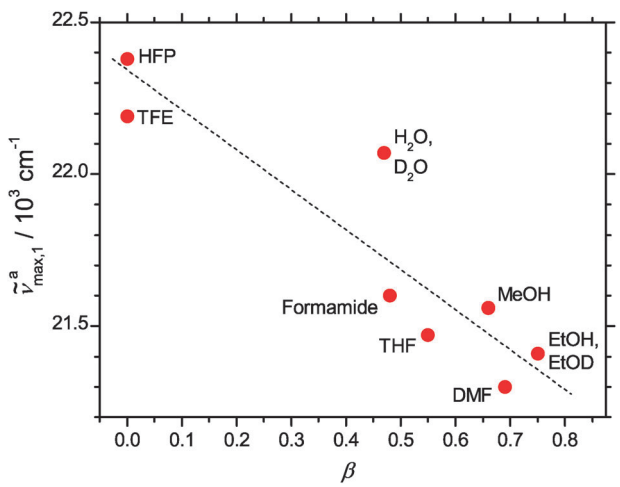

Fig. 9 Dependence of the position of the $S_0 \rightarrow S_1$ absorption maximum (Table 1) of ATTO 465 on the Kamlet–Taft parameter β for different solvents. The dashed line is intended merely as a guide to the eye.

We now turn toward the variations in temperature dependence depicted in Fig. 5. Somewhat surprising is the increase in the lifetime with increasing temperature observed for ethanol and methanol in the TCSPC experiments, whereas the lifetime decreases in water. The fact that the lifetimes are hardly affected by the pH value suggests that acid–base equilibria of the dye are likely not responsible for the observed trends. A reasonable explanation for the experimental results can be found by invoking the so-called "proximity effect": as originally described by Lim and co-workers, many nitrogen-containing heterocyclic compounds and aromatic carbonyl derivatives show a characteristic solvent and temperature dependence of their excited-state lifetimes and fluorescence quantum yields.[41–46] This behavior is thought to arise from vibronic interactions between two close-lying $n\pi^*$ and $\pi\pi^*$ states. For instance, in the case of psoralens, an increase in the excited-state lifetime was observed with increasing solvent polarity, and it was particularly large in highly polar hydrogen-bonding solvents:[41,44] in this case, the polarity of the solvent influences the energy gap between the two states. Specifically $\pi\pi^*$ is more strongly stabilized with respect to $n\pi^*$ in polar solvents, reducing the proximity effect and therefore the IC rate constant.[41] An increase in temperature increases the excitation of vibronically active modes, which enhance the proximity effect and accelerate IC.[41]

Such a proximity effect could explain many trends observed for ATTO 465: the dye also features two close-lying electronic singlet states (see Table 2), and the longest lifetime is observed for highly polar solvents with small β parameter, which would correspond to the case with the largest energy gap.[45,47] Also, the increase in the IC rate constant with temperature for water can be understood in the framework of this model. The unusual "inverse" temperature dependence for methanol and ethanol might then be the result of subtle effects, such as a reversal of the state ordering upon an increase in temperature, which becomes possible because the two states should be closer in energy in these solvents.[42] The situation might become even more complex when invoking temperature and solvent dependent complexation equilibria. As an indication for this we take the aforementioned shifts in the steady-state absorption and fluorescence spectra, which suggest that there are considerable changes in solvation with variation of the solvent which correlate with the β parameter (Fig. 9). In such a case, "more complexed" and "less complexed" forms could exhibit different lifetimes which affect the temperature dependent effective lifetimes observed in the different solvents.

The final point raised at the start of this section concerns the fast initial decay of ~16 ps visible in the PSCP spectra of water (Fig. 8(C) and (D)). These spectral dynamics cannot be due to some relaxation process within the excited state, because this should only affect the ESA and SE features. Instead, the fast decay is observed throughout the entire spectrum (including the S_0 GSB, Fig. 8(D)). One possible explanation could be the presence of ATTO 465 dimers which quickly relax back to S_0. To investigate this point, additional time-resolved experiments in water were carried out at different ATTO 465 concentrations on a separate transient absorption setup, where a higher signal-to-noise ratio

can be obtained (λ_{pump} = 430 nm, λ_{probe} = 860 nm). Kinetic traces are shown in Fig. S5 (ESI†). Changing the concentration by a factor of 10 did not have an impact on the transients, and the fast decay remained unchanged. Therefore we believe that we can rule out an influence of ATTO 465 dimers. Another explanation for the fast decay could be that after photoexcitation to S_1, a fraction of the ATTO 465 molecules populate the close-lying almost dark electronic state (see Table 2). Molecules in this state would then, independently of S_1, quickly return to S_0 by nonradiative relaxation.

5. Conclusions

The 3,6-diaminoacridinium dye ATTO 465 shows interesting photophysical features. Unusual properties, such as the prominent blue-shift and broadening of the absorption spectra in water, a protic ionic liquid and two fluorinated alcohols as well as the increase in the S_1 lifetime with increasing temperature in ethanol and methanol (but not in water) should be noted in this respect. The experimental observations can be reasonably well explained on the basis of a ''proximity effect'' originating from the closely spaced S_1 and S_2 states. The solvent polarity and temperature dependent energy gap between the two states affect the excited-state lifetime. In addition, temperature-dependent equilibria between more or less solvent-complexed forms of ATTO 465 may also have an influence on the lifetime.

In the future it would be worthwhile to investigate this system using fluorescence up-conversion techniques to elucidate the origin of the fast decay component in water. In addition, we are currently carrying out CASPT2 calculations to obtain more accurate data for the location and ordering of the electronic states.

The photophysical features of ATTO 465 might become beneficial for probing hydrogen-bond interactions either *via* the pronounced changes in the steady-state absorption and fluorescence properties or changes in the lifetime of the dye. In this way, covalently linked ATTO 465 derivatives could be utilized as molecular probes for peptide and protein folding processes in protic ionic liquids. Research along these lines is currently also pursued in our laboratories.

Acknowledgements

We would like to thank N. P. Ernsting and J. L. Pérez Lustres for their help during the implementation of the PSCP setup, and J. Troe and A. M. Wodtke for on-going generous support. Thanks go also to D. Imhof for valuable discussions. In addition, we acknowledge excellent technical assistance by D. Gaumann, B. Meyer and M. Rabe. We would also like to thank the referees for very helpful comments and suggestions. K. Oum and T. Lenzer are grateful to the German Research Foundation for funding of this work within the Priority Programme SPP 1191 ''Ionic Liquids''.

Notes and references

1 H. W. Zimmermann, *Angew. Chem., Int. Ed. Engl.*, 1986, **25**, 115 (*Angew. Chem.*, 1986, **98**, 115).
2 A. Chmyrov, J. Arden-Jacob, A. Zilles, K.-H. Drexhage and J. Widengren, *Photochem. Photobiol. Sci.*, 2008, **7**, 1378.
3 K. S. Kumar, C. Selvaraju, E. J. P. Malar and P. Natarajan, *J. Phys. Chem. A*, 2012, **116**, 37.
4 ATTO-TEC Fluorescent Labels and Dyes, Catalogue 2011–2013.
5 T. L. Greaves and C. J. Drummond, *Chem. Rev.*, 2008, **108**, 206.
6 A. Miloslavina, C. Ebert, D. Tietze, O. Ohlenschläger, C. Englert, M. Görlach and D. Imhof, *Peptides*, 2010, **31**, 1292.
7 M.-M. Huang and H. Weingärtner, *ChemPhysChem*, 2008, **9**, 2172.
8 W. H. Melhuish, *J. Phys. Chem.*, 1961, **65**, 229.
9 K. A. Zachariasse, G. Duveneck and R. Busse, *J. Am. Chem. Soc.*, 1984, **106**, 1045.
10 U. Leinhos, W. Kühnle and K. A. Zachariasse, *J. Phys. Chem.*, 1991, **95**, 2013.
11 P. W. Lohse, J. Kuhnt, S. I. Druzhinin, M. Scholz, M. Ekimova, T. Oekermann, T. Lenzer and K. Oum, *Phys. Chem. Chem. Phys.*, 2011, **13**, 19632.
12 A. L. Dobryakov, S. A. Kovalenko, A. Weigel, J. L. Pérez Lustres, J. Lange, A. Müller and N. P. Ernsting, *Rev. Sci. Instrum.*, 2010, **81**, 113106.
13 T. Lenzer, S. Schubert, F. Ehlers, P. W. Lohse, M. Scholz and K. Oum, *Arch. Biochem. Biophys.*, 2009, **483**, 213.
14 K. Oum, P. W. Lohse, F. Ehlers, M. Scholz, M. Kopczynski and T. Lenzer, *Angew. Chem., Int. Ed.*, 2010, **49**, 2230 (*Angew. Chem.*, 2010, **122**, 2277).
15 K. Golibrzuch, F. Ehlers, M. Scholz, R. Oswald, T. Lenzer, K. Oum, H. Kim and S. Koo, *Phys. Chem. Chem. Phys.*, 2011, **13**, 6340.
16 A. D. Becke, *J. Chem. Phys.*, 1993, **98**, 5648.
17 E. Runge and E. K. U. Gross, *Phys. Rev. Lett.*, 1984, **52**, 997.
18 A. Dreuw and M. Head-Gordon, *Chem. Rev.*, 2005, **105**, 4009.
19 M. J. Frisch, G. W. Trucks, H. B. Schlegel and G. E. Scuseria, *et al.*, *Gaussian 09, Revision A.01;* Gaussian, Inc.: Wallingford, CT (USA), 2009.
20 Y. Shao, L. Fusti-Molnar, Y. Jung and J. Kussmann, *et al.*, *Phys. Chem. Chem. Phys.*, 2006, **8**, 3172.
21 Y. Marcus, *Chem. Soc. Rev.*, 1993, 409.
22 S. Spange, R. Sens, Y. Zimmermann, A. Seifert, I. Roth, S. Anders and K. Hofmann, *New J. Chem.*, 2003, **27**, 520.
23 *Handbook of Chemistry and Physics*, 85 edn, ed. D. R. Lide, CRC Press, Boca Raton, 2004.
24 E. Koglin and J.-M. Séquaris, *J. Mol. Struct.*, 1986, **141**, 405.
25 M. Schreiber, V. Buß and M. P. Fülscher, *Phys. Chem. Chem. Phys.*, 2001, **3**, 3906.
26 D. Jacquemin, E. A. Perpète, G. Scalmani, M. J. Frisch, R. Kobayashi and C. Adamo, *J. Chem. Phys.*, 2007, **126**, 144105.
27 D. Jacquemin, V. Wathelet, E. A. Perpète and C. Adamo, *J. Chem. Theory Comput.*, 2009, **5**, 2420.
28 R. Battino, T. R. Rettich and T. Tominaga, *J. Phys. Chem. Ref. Data*, 1983, **12**, 163.
29 U. Hold, T. Lenzer, K. Luther and A. C. Symonds, *J. Chem. Phys.*, 2003, **119**, 11192.

30 M. Kopczynski, F. Ehlers, T. Lenzer and K. Oum, *J. Phys. Chem. A*, 2007, **111**, 5370.
31 S. I. Druzhinin, A. Demeter, V. A. Galievsky, T. Yoshihara and K. A. Zachariasse, *J. Phys. Chem. A*, 2003, **107**, 8075.
32 S. I. Druzhinin, Y.-B. Jiang, A. Demeter and K. A. Zachariasse, *Phys. Chem. Chem. Phys.*, 2001, **3**, 5213.
33 C. Wohlfarth and B. Wohlfarth, *Landolt-Börnstein – Vol. IV/6, Static Dielectric Constants of Pure Liquids and Binary Liquid Mixtures*, Springer, Berlin, Heidelberg, 1991.
34 M. L. Horng, J. A. Gardecki, A. Papazyan and M. Maroncelli, *J. Phys. Chem.*, 1995, **99**, 17311.
35 P. W. Lohse, F. Ehlers, K. Oum, M. Scholz and T. Lenzer, *Chem. Phys.*, 2010, **373**, 45.
36 T. Lenzer, F. Ehlers, M. Scholz, R. Oswald and K. Oum, *Phys. Chem. Chem. Phys.*, 2010, **12**, 8832.
37 B. Soep, A. Kellmann, M. Martin and L. Lindqvist, *Chem. Phys. Lett.*, 1972, **13**, 241.
38 M. Sajadi, M. Weinberger, H.-A. Wagenknecht and N. P. Ernsting, *Phys. Chem. Chem. Phys.*, 2011, **13**, 17768.
39 D. Schwarzer, J. Troe, M. Votsmeier and M. Zerezke, *J. Chem. Phys.*, 1996, **105**, 3121.
40 S. Spange, S. Prause, E. Vilsmeier and W. R. Thiel, *J. Phys. Chem. B*, 2005, **109**, 7280.
41 T.-i. Lai, B. T. Lim and E. C. Lim, *J. Am. Chem. Soc.*, 1982, **104**, 7631.
42 T.-i. Lai and E. C. Lim, *J. Am. Chem. Soc.*, 1985, **107**, 1134.
43 E. C. Lim, *J. Phys. Chem.*, 1986, **90**, 6770.
44 G. G. Gurzadyan, *Photochem. Photobiol. Sci.*, 2002, **1**, 757.
45 P. S. Sherin, J. Grilj, Y. P. Tsentalovich and E. Vauthey, *J. Phys. Chem. B*, 2009, **113**, 4953.
46 A. Kobayashi, K. Takehira, T. Yoshihara, S. Uchiyama and S. Tobita, *Photochem. Photobiol. Sci.*, 2012, **11**, 1368.
47 M. Kasha, in *Light and Life*, ed. W. D. McElroy and B. Glass, John Hopkins University Press, Baltimore, MD, 1961, p. 31.